

Article

Microfluidic Simulation and Optimization of Blood Coagulation Factors and Anticoagulants in Polymethyl Methacrylate Microchannels

Philip Nathaniel Immanuel ^{1,*}, Yi-Hsiung Chiu ^{2,†} and Song-Jeng Huang ^{1,*} 

¹ Department of Mechanical Engineering, National Taiwan University of Science and Technology, Taipei 106, Taiwan

² Pacific Engineers & Constructors, Ltd. (PECL), Taipei 106, Taiwan; elisha0524@gmail.com

* Correspondence: d10603816@gapps.ntust.edu.tw (P.N.I.); sgjhuang@mail.ntust.edu.tw (S.-J.H.)

† These two authors contributed equally to this work.

Abstract: Blood coagulation is a critical and complex reaction that involves various chemical substances, such as prothrombin, fibrinogen, and fibrin. The process can be divided into three main steps, namely the formation of the prothrombin activator, conversion of prothrombin to thrombin, and conversion of fibrinogen to fibrin. In this study, an ANSYS simulation is carried out to determine the prothrombin time (PT) of blood, the chemical changes that occur during coagulation and the anticoagulation factor. The addition of deionized water to the microchannels before the addition of blood and reagents results in a two-phase flow. The evaluation of this two-phase flow is necessary, and dynamic simulations are required to determine the PT. The chemical rate constant and order of the chemical reaction are derived from the actual prothrombin time. Moreover, the genetic algorithms in PYTHON and ANSYS are used to estimate chemical reaction parameters for a 20 s PT. The blood and anticoagulant exhibit increased dynamic behavior in the microchannel. In addition, particles are added to the microchannel and the dynamic mesh method is used to simulate the flow behaviors of the red and white blood cells in the microchannel. The PTs for different volumes of blood are also reported.

Keywords: microchannels; simulation; anticoagulants; chemical reaction; two phase flow; genetic algorithm; dynamic mesh



Citation: Immanuel, P.N.; Chiu, Y.-H.; Huang, S.-J. Microfluidic Simulation and Optimization of Blood Coagulation Factors and Anticoagulants in Polymethyl Methacrylate Microchannels. *Coatings* **2021**, *11*, 1394. <https://doi.org/10.3390/coatings11111394>

Academic Editor: Rahmat Ellahi

Received: 18 October 2021

Accepted: 8 November 2021

Published: 15 November 2021

Publisher's Note: MDPI stays neutral with regard to jurisdictional claims in published maps and institutional affiliations.



Copyright: © 2021 by the authors. Licensee MDPI, Basel, Switzerland. This article is an open access article distributed under the terms and conditions of the Creative Commons Attribution (CC BY) license (<https://creativecommons.org/licenses/by/4.0/>).

1. Introduction

Recent statistics tell us that the aging of the population has already become a major social issue in several countries, making it necessary to monitor the health of older people. An aging population brings with it an increased risk of several illnesses common to older individuals, such as various types of cancer, cardiovascular, bleeding and metabolic diseases, and severe infections [1–4]. In addition, the severity of such diseases is higher in elders than in younger people. Therefore, the detection of health risk in the early stages is necessary to preserve the health of this portion of the population. Severe bleeding that causes death are bleeding inside the skull (intracranial), subarachnoid, and rupture. Blood coagulation and platelet defects are the causes of bleeding that lead to death [4]. In order to prevent this, understanding the chemical reaction that occurs during blood coagulation and finding the chemical reaction rate involved in the coagulation process are necessary. For this purpose, a new microfluidic device has been devised to detect the blood clotting time (coagulation time) to assist in the early detection of cardiovascular diseases and bleeding disorders.

Several studies have investigated the blood flow in microchannels for drug delivery [5–7]. Some studies have examined the microfluidic flow field structures and mixing performance in the microchannels of such devices [8–12]. Jafari et al. reports the optimized

parameter of heat sinks fluid flow microchannel using a genetic algorithm, which states the volume flow rate ranges from 0.005 to 0.009 m³/s and the entropy generation rate is minimized. Therefore, genetic algorithm can be optimized for unknown parameters to obtain better results [13]. The inertial force of fluid is small due to the diameter of the microfluidic channel, which is on the order of 10⁻⁶ m, resulting in a Reynolds number between 0.01 and 100 [8]. Under this Reynolds number condition, laminar flow of the fluid occurs in the microchannel. Fluids can be mixed into this flow only through diffusion. In biomedical testing, increasing the efficiency of the mixing of fluid with the sample and the reagent pretreatment is necessary. In this work, we use species transport and chemical reaction, which involves an unknown reaction rate constant and reaction order, and use a genetic algorithm to calculate these parameters.

Substances involved in the coagulation process are collectively referred to as coagulation factors [14]. Blood coagulation is a complex process which involves 14 different steps that can be roughly divided into three chemical reactions, namely, the formation of a prothrombin activator, prothrombin to thrombin conversion, and fibrinogen to fibrin conversion. Under normal circumstances, the coagulation reaction is rapid, using an internal cascade mechanism to amplify the coagulation signal step by step, and positive feedback links to enhance the coagulation process. In addition, the coagulation mechanisms during hemostasis combine (especially the platelet thrombosis mechanisms) to reinforce and promote each other. To prevent accidental thrombosis under normal conditions and to control the thrombus formed at the bleeding site, the body triggers anticoagulant and fibrinolysis mechanisms against the coagulation mechanism [15,16].

Since generic algorithms have been demonstrated to be an effective technique for optimization and finding better solutions, they are used in this study to calculate the coagulation reaction coefficient. Here, we simulate and calculate the PT chemical reaction rate of the blood, as well as report the point of care (POC) PT time.

2. Methodology

A microfluidic chip (length 100 mm × width 100 mm) including a microchannel of 1 mm diameter was modeled and analyzed in this work, which was adopted from Manda et al. [17]. The microchannel exhibits two inlet and an outlet, and its substrate is made of polymethyl methacrylate (PMMA). Reagent and blood were used as a reactant for the calculation of PT time and the chemical reaction rate constants in the microchannel. The model of microfluidic chip and its dimension are presented in Figure 1.

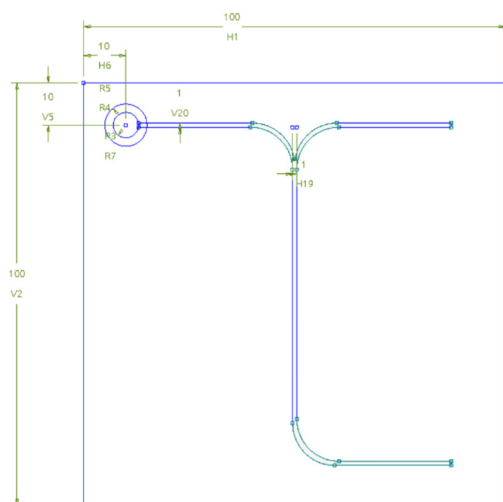


Figure 1. Model structure of microfluidic chip with microchannel.

Computational fluid dynamics [18] are used to simulate and observe the mixing of blood and reagents in the mixed-flow field in a microchannel. The convection diffusion

equation and a series of chemical reaction equations for blood coagulation are introduced as the source/sink term for the equation. Moreover, appropriate initial and boundary conditions are applied. A numerical simulation is carried out to analyze the reaction process between the reagent and the blood sample in the microchannel for analysis of the chemical reaction and evaluation of the mixing process.

The genetic algorithm method involves the following steps [19]: (1) generate a set of starting values for a parallel search to avoid the local minimum- or maximum-value loop; (2) use probabilistic selection rules rather than deterministic rules; (3) calculation is mainly performed by the coding of the chromosome rather than the parameters themselves; (4) obtain the fitness score by using the objective function rather than other derivative or auxiliary information. Some studies have suggested using genetic algorithm methods for optimization of the transport behavior of microchannel heat transfer and mass transfer [20,21]. However, since ANSYS Fluent does not provide this feature, we used PYTHON to develop the genetic algorithm. The interactive calculation with ANSYS Fluent is depicted in Figure 2.

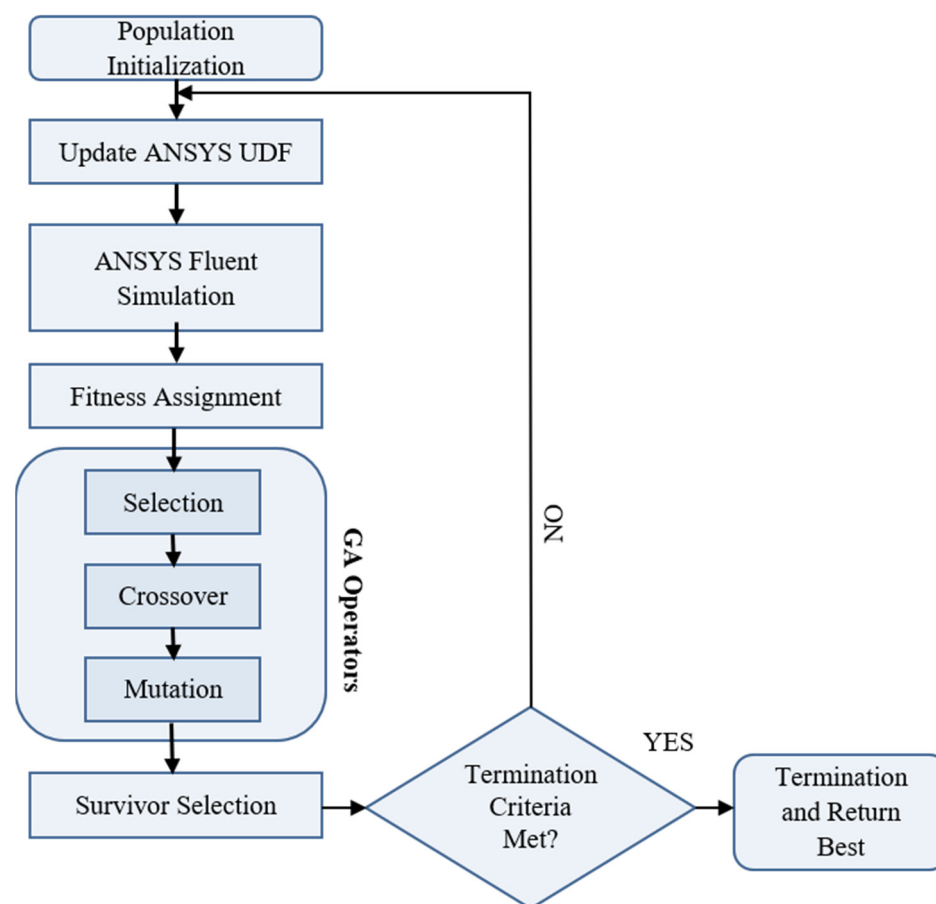


Figure 2. Flow chart of the genetic algorithm.

An efficient dynamic mesh technique [18], which can be used to simulate the problem of flow field variation with respect to time and boundary motion, can be devised using the ANSYS Fluent dynamic mesh model. The motion of the boundary can be rigid or deformed. It can be a predefined motion or a motion that is not defined in advance. During simulation, the mesh update is automatically performed using ANSYS Fluent according to the changes in the boundaries of each iteration step. Dynamic meshes have also been used in several studies to simulate the flow of blood in blood vessels [22–24].

3. Governing Equations and Boundary Conditions

To prevent the microchannel from being contaminated by impurities and dust, pure water (DI water) is first introduced into the microchannel before the addition of the blood and reagent. This creates a two phase flow. The blood and reagent are mixed in one phase, and the pure water flow is the other phase. Therefore, the Eulerian–Eulerian method is used to simulate the two phases as continuous fluids. The conservation equation is mainly applied to the blood sample and reagent phase [18] (ANSYS 2019).

3.1. Equation of Continuity

$$\frac{\partial(\alpha_i \rho_i)}{\partial t} + \nabla \cdot (\alpha_i \rho_i \vec{V}_i) = \pm \dot{m}_{ij} \quad (1)$$

where the density is mixed by volume weight as follows:

$$\rho = \frac{1}{\sum_i \frac{Y_i}{\rho_i}} \quad (2)$$

3.2. Momentum Equation

$$\frac{\partial(\alpha_i \rho_i \vec{V}_i)}{\partial t} + \nabla \cdot (\alpha_i \rho_i \vec{V}_i \vec{V}_i) = -\alpha_i \nabla P_i + \alpha_i \cdot \tau_i + \alpha_i \rho_i g + \beta (\vec{V}_i - \vec{V}_j) \quad (3)$$

where the stress tensor τ_i is expressed as follows:

$$\tau_i = \alpha_i \mu_i \left[\vec{V}_i + (\vec{V}_i)^T \right] - \frac{2}{3} \alpha_i \mu_i (\vec{V}_i) \quad (4)$$

The viscosity can be obtained by mass weight mixing as follows:

$$\mu = \sum_i \frac{X_i \mu_i}{\sum_j X_j \phi_{ij}} \quad (5)$$

$$\phi_{ij} = \frac{\left[1 + \left(\frac{\mu_i}{\mu_j} \right)^{1/2} + \left(\frac{M_{w,j}}{M_{w,i}} \right)^{1/4} \right]^2}{\left[8 \left(1 + \frac{M_{w,j}}{M_{w,i}} \right) \right]^{1/2}} \quad (6)$$

3.3. Species Transport Equations

$$\frac{\partial(\rho_i Y_j)}{\partial t} + \nabla \cdot (\rho_i \vec{V}_i Y_j) = -\nabla \cdot J_j + R_j + S_j \quad (7)$$

where the diffusion flux J_j and the chemical reaction rate R_j are expressed as follows:

$$J_j = \rho D_{j,m} \nabla Y_j \quad (8)$$

$$R_j = M_{w,j} \sum_{r=1}^{N_r} \hat{R}_{j,r} \quad (9)$$

The general formula for the chemical reaction is as follows:

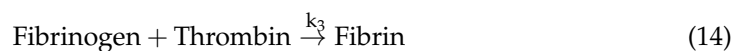
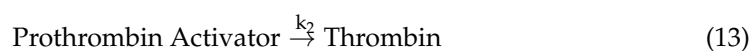
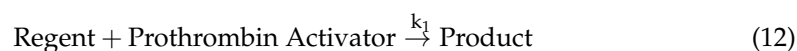


For the aforementioned reaction formula, the reaction rate or rate of formation of the substance k in the reaction r can be derived as follows:

$$\hat{R}_{j,r} = \Gamma \left(v''_{j,r} - v'_{j,r} \right) \left\{ k_{f,r} \prod_{k=1}^{N_r} [C_{k,r}]^{n'_{k,r}} - k_{b,r} \prod_{k=1}^{N_r} [C_{k,r}]^{n''_{k,r}} \right\} \quad (11)$$

According to Seegers et al., blood coagulation can be mainly divided into three main stages [16].

As mentioned earlier, the formation reaction of the prothrombin activator is a complex reaction. The prothrombin activator is assumed to have a constant value in the present study. In addition, the prothrombin activator reacts with a reagent (anticoagulant). Therefore, the chemical reaction can be simplified as follows:



The chemical reaction rate can be expressed as follows:

$$R_1 = k_1 C_R^{n_1} C_{PA}^{n_2} \quad (15)$$

$$R_2 = k_2 C_{PA}^{n_3} \quad (16)$$

$$R_3 = k_3 C_{FG}^{n_4} C_T^{n_5} \quad (17)$$

where R is a reagent (anticoagulant); PA is the prothrombin activator; T is thrombin; and FG is fibrinogen.

The objective function is used to estimate the chemical reaction parameters. Therefore, in this study, the objective function is set as the minimum value of the average mass fraction of the prothrombin activator and fibrin at the end of the microchannel, as presented in Equation (18) [18].

$$\text{Objective function} = \sum_{i=1}^Q f_i \frac{\iint w_i dA}{\iint dA} \quad (18)$$

where f_i is an objective function coefficient corresponding to the i^{th} variable; dA is the average mass fraction of the prothrombin activator and fibrin; and w_i is the weighting mass fraction of the prothrombin activator and fibrin. The following parameters are selected for the genetic algorithm: population size of 100; chromosome length of 10; crossover probability of 0.75; and mutation probability of 0.05. In addition, to simulate the flow of red blood cells (RBC) and white blood cells (WBC) inside the microchannel, particles are added to the flow field. Moreover, the transport behavior of the particles in the microchannel is observed using the dynamic mesh technique and Newton's second and third laws of motion. In this study, to reduce the convergence time and complexity of the simulation, the particles are divided into three groups. Each group has approximately 3–10 RBCs, and the groups do not affect each other.

3.4. Boundary Equations

Since the microfluidic channel is filled with DI water at the beginning of the process, if the inlet flow rate is less than a certain value, blood or reagent cannot flow in the microfluidic channel. Therefore, the inlet speed of the blood and reagent is set to 0.005 m/s. The condition between the microchannel and the wall is assumed to be no-slip. In addition, the prothrombin activator and fibrinogen contents in the blood are assumed to be 0.01 and 0.04 wt%, and the other inlet is a reagent, respectively.

4. Results and Discussion

The reference value for the prothrombin time (PT) varies depending on the analytical method used but is generally approximately 12–13 s. For subjects who have not received anticoagulation therapy, the international normalized ratio (INR) reference value is 0.8–1.2. If anticoagulant drugs are used, the INR value can be 2–3 [25]. Therefore, in this study, a dynamic simulation is used to investigate changes in the blood and anticoagulant in the microchannel.

Figure 2 shows a flow chart of the genetic algorithm. We first discuss the distribution of the mass fraction for each item in the flow channel with various k_1 – k_3 and n_1 – n_5 values after 20 s, because different k_1 – k_3 and n_1 – n_5 values affect the prothrombin activator, thrombin, and fibrin contents in the microchannel. The small area in the panel on the left-hand side of Figure 3 indicates that the blue zone contains the blood inlet side and mixing area. The brown zone is the reagent inlet side, which indicates that the mass fraction of the prothrombin activator decreases because the k_1 and n_1 values are small. The rate of decrease of n_1 is higher than that of k_1 . Figure 3 shows that initially the prothrombin activator in blood side and mass fraction is 100% before the reaction; then, prothrombin gradually descends in the microfluidic channel. At $x = 0$, it immediately reacts with the reagent, so the reaction is complete before $x < 5$. Since the prothrombin reaction is related to R1 (Equation (18)), the k_1 and n_1 will affect the time of prothrombin activator in the microchannel. From Figure 3, it can be found that when n_1 is equal to 2.0, the reagent will flow to the blood side and react with prothrombin rapidly, hence it will complete reaction when $x < 5$. As can be seen in Figure 4, the tendency of the thrombin content to decrease after an increase in response does not occur in the mixed zone. Therefore, it is speculated that the prothrombin activator has completely reacted with thrombin before it enters the mixed zone. The larger the k_1 value and the smaller the n_3 value, the slower the rate of thrombin formation in the flow channel. As indicated on the left of Figure 4, the increase in magnitude when $k_1 = 0.1$ and 0.001 is almost the same as for 1.0 and 0.1, indicating that there should be a limiting value for k_1 . As depicted on the right of Figure 4, the maximum value is obtained at $x = -10$ mm when $n_3 = 2$, which indicates that the values of k_1 and n_3 have a considerable effect on the distribution of thrombin in the microchannel. According to Equation (17), the thrombin content is proportional to the fibrin content. Thrombin is the intermediate product of prothrombin and fibrinogen. Prothrombin activator starts to produce thrombin in the blood side of the microchannel at the beginning. When the reagent and the prothrombin activator react completely, the thrombin will react only with fibrinogen, hence thrombin will decrease in the microchannel. When $n_3 = 2$, which indicates that thrombin will react with fibrinogen to produce fibrin, hence, the thrombin will decrease at $x > 0$. As depicted on the left in Figure 5, when $k_2 = 0.001$, the rate of thrombin generation is low, which results in the fibrin mass fraction being almost equal to 0. Conversely, part of the thrombin content continues to react to form fibrin in the mixed zone when $k_2 = 0.1$. When $x < 0$, the fibrin mass fraction increases along with the microchannel, and when it is not mixed with reagents and chemical reaction ($x > 0$), it starts to decrease along the microchannel.

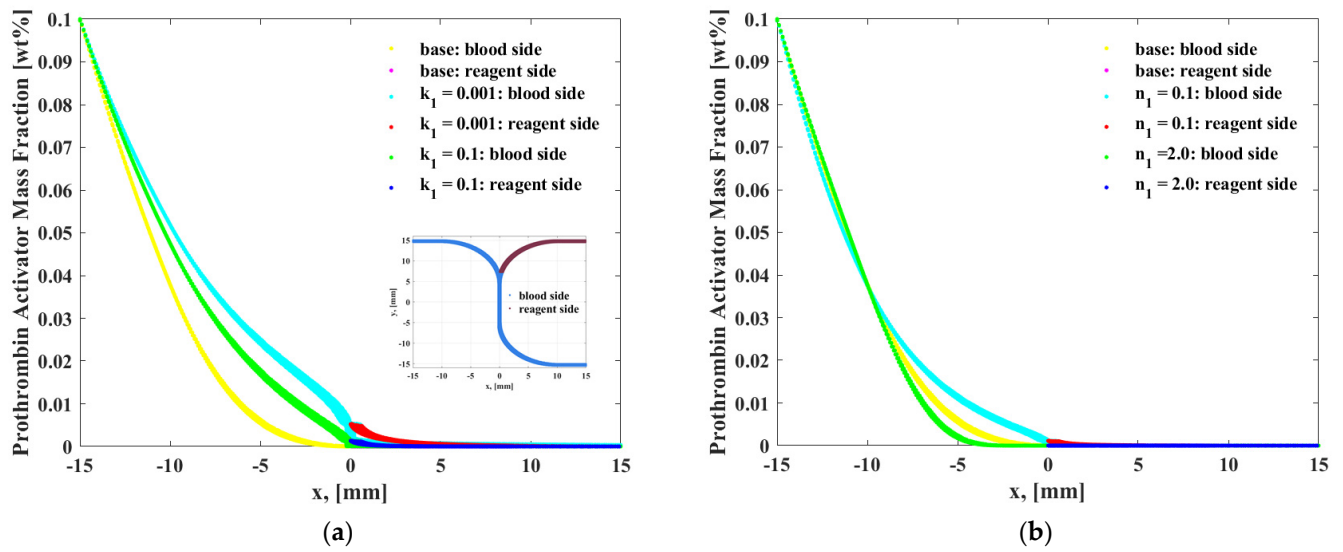


Figure 3. Distribution of the mass fraction of the prothrombin activator for (a) various k_1 and (b) n_1 .

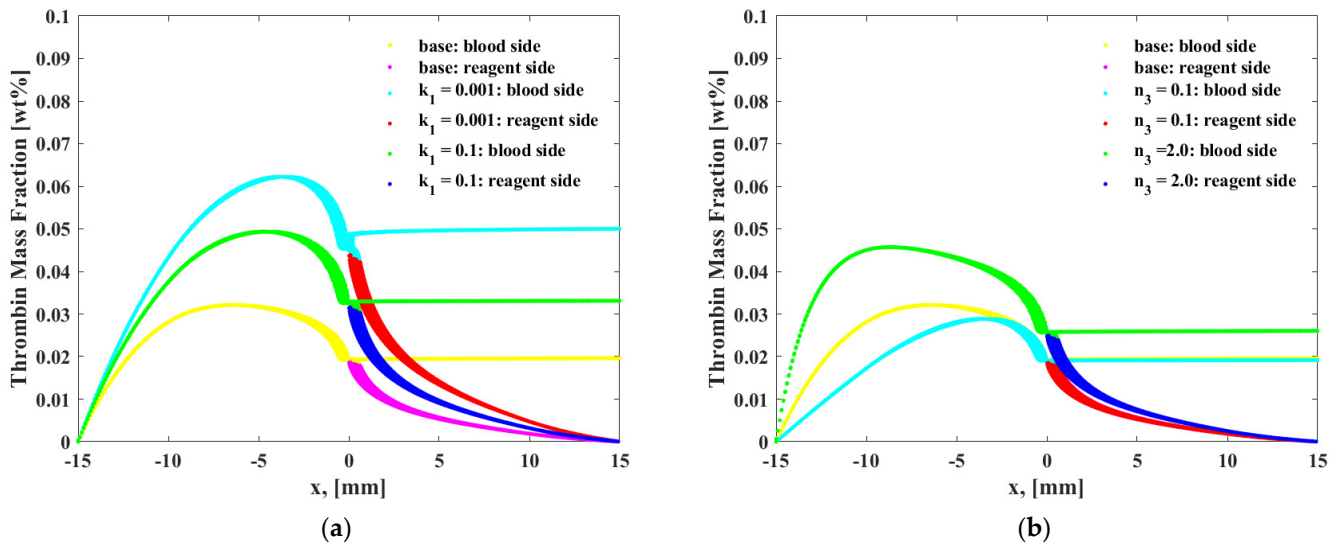


Figure 4. Distribution of the mass fraction of thrombin for (a) various k_1 and (b) n_3 .

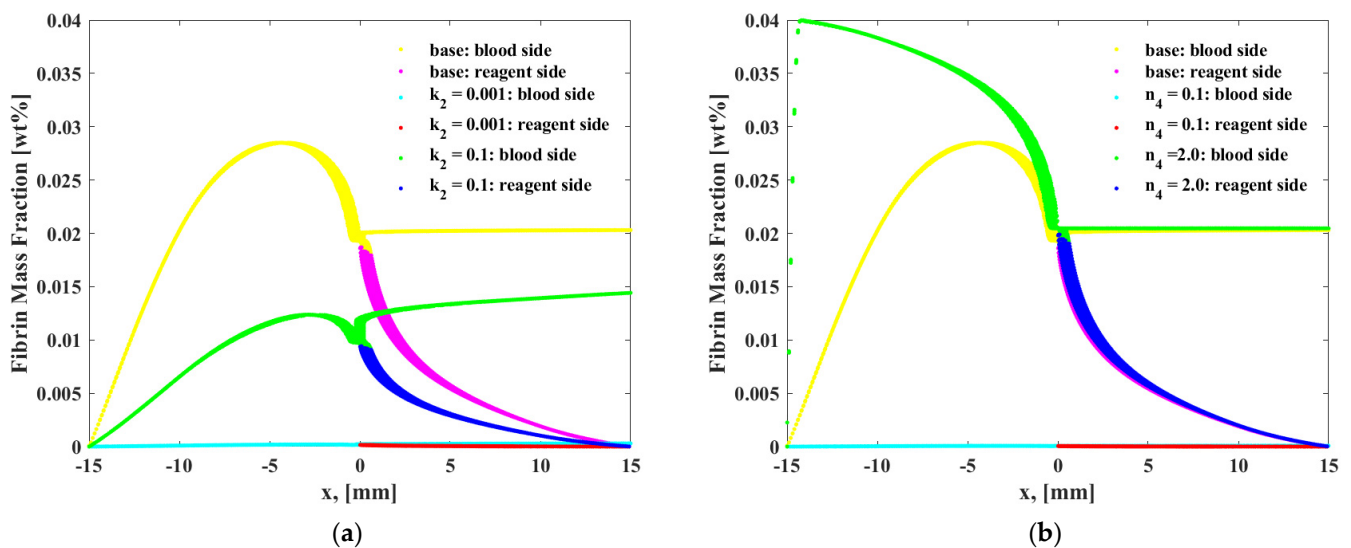


Figure 5. Distribution of the mass fraction of fibrin for (a) various k_2 and (b) n_4 .

In this study, the parameters k_1 – k_3 obtained using the genetic algorithm were 0.987, 0.43, and 0.877, respectively, and those obtained for n_1 – n_5 were 0.548, 1.631, 1.23, 0.459, and 1.341, respectively. These results are indicative of the behavior of the prothrombin activator and fibrin in the microchannel. As can be seen in Figure 6, the chemical reaction with the anticoagulant does not occur at 1 s, because the prothrombin activator has yet to enter the mixed zone at this time. The prothrombin activator reacts with the anticoagulant within 3–5 s, and the reaction rate is high. Although a high prothrombin activator content is present in the blood at the side channel at 3 s, the activity of the prothrombin activator decreases after 5 s. Finally, the mass fraction of the prothrombin activator is nearly stable.

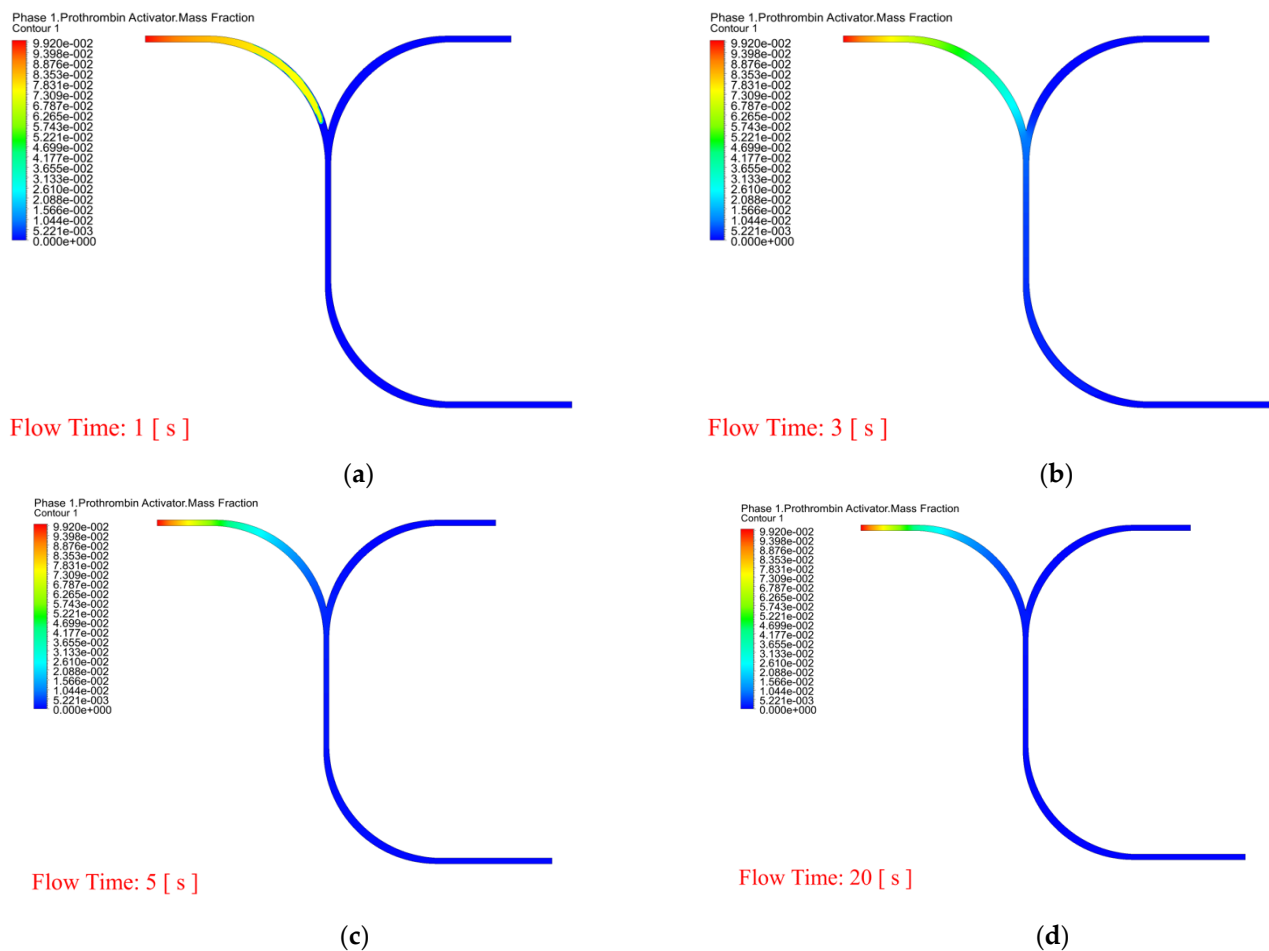


Figure 6. Mass fraction of the prothrombin activator in the microchannel at various times (a) 1 s, (b) 3 s, (c) 5 s, and (d) 20 s.

As indicated by Equations (16) and (17), thrombin and fibrin in the blood undergo spontaneous reactions and a proportional relationship exists between them. The fibrin reaction has already begun before entering the mixed zone (Figure 7). A slowdown in the fibrin flow speed occurs at 3 s in the microfluidic channel because of the high viscosity of fibrin [21], which causes thrombin and fibrin to flow out of the microchannel after 5 s. In addition, the reaction extends to the reagent channel side, except in the mixed region.

Figure 8 depicts the average mass fraction of each component in the microchannel as a function of time. The prothrombin activator enters the mixing zone and reacts rapidly with the anticoagulant to produce a chemical reaction at 1.2 s, and its content then quickly decreases with time. Almost no chemical reaction occurs in the microchannel. In addition, the fibrin reaction is rapid and tends to stabilize at approximately 4 s.

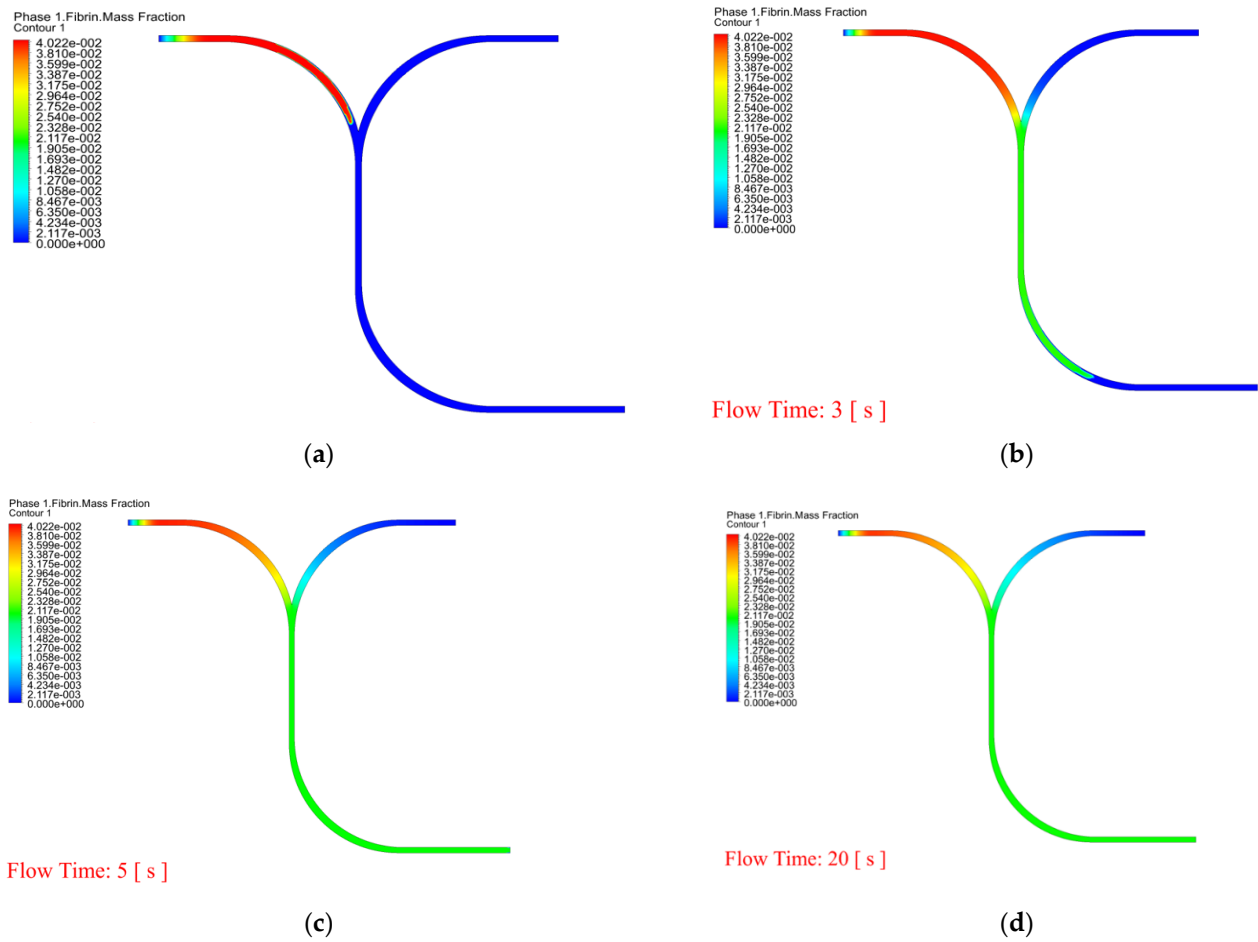


Figure 7. Mass fraction of fibrin in the microchannel at various times (a) 1 s, (b) 3 s, (c) 5 s, and (d) 20 s.

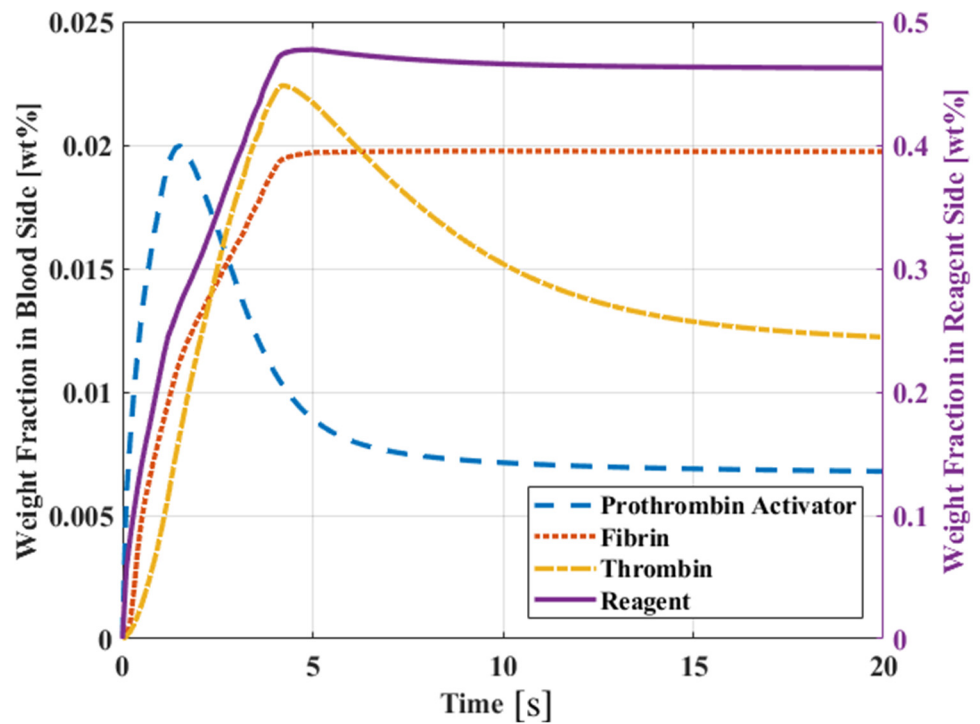


Figure 8. Average species weight fraction in the blood and reagent sides.

The flow condition in which the RBCs and WBCs pass through the microchannel is illustrated in Figure 9. The RBCs and WBCs are ready to enter the mixing zone at approximately 4.3 s, as illustrated in Figure 8. The chemical reaction rapidly generates a large amount of fibrin, thereby decreasing the flow velocity of particles in the microchannel. In addition, the time it takes for microparticles to flow out of the micro passage increases, because the passing particles collide with the curved surface of the wall and rebound. As can be seen in the figure, the particles flow completely out of the micro flow channel after 11.7 s.

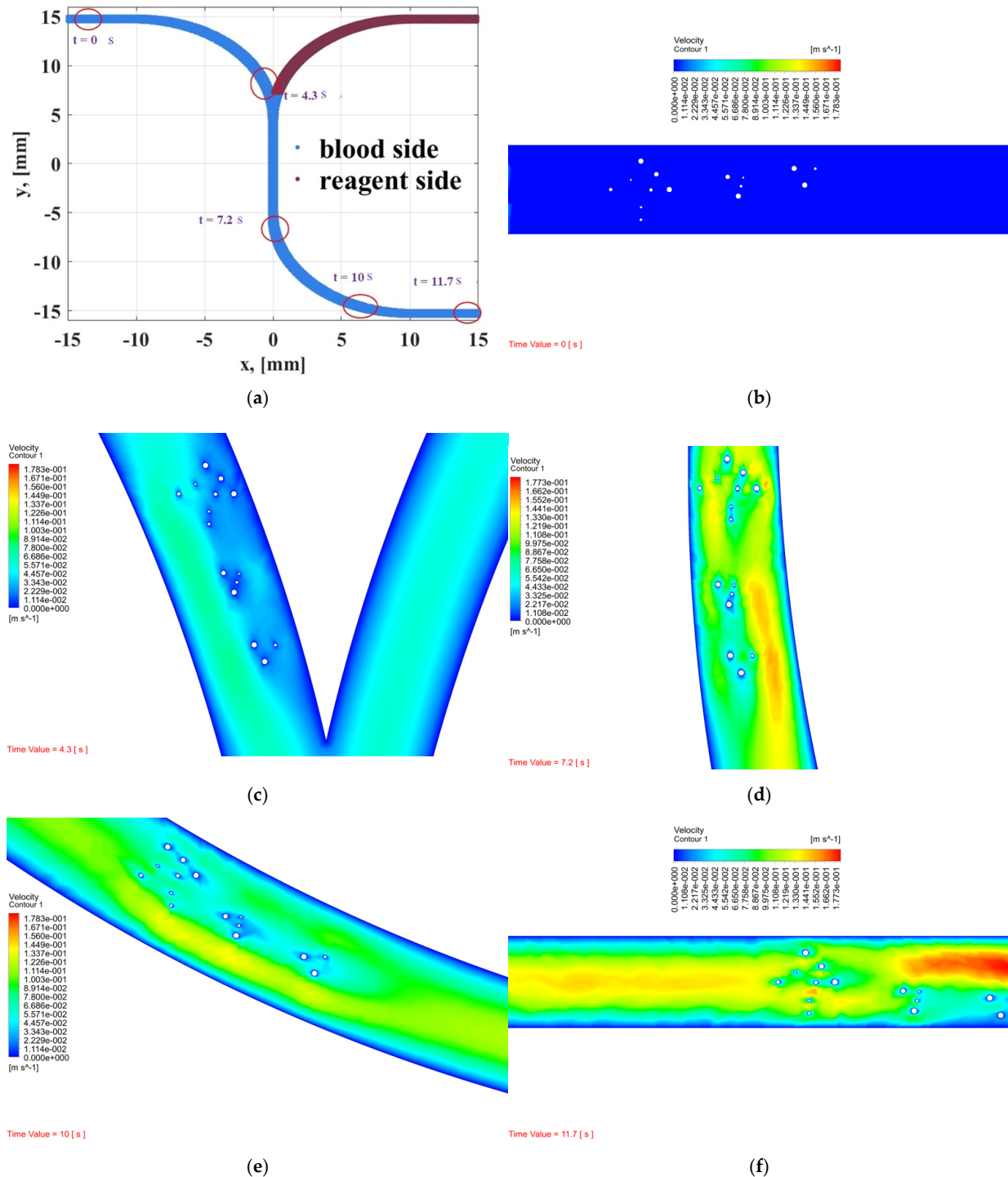


Figure 9. Dynamic behavior of WBCs and RBCs in the microchannel of (a) whole flow, (b) 0 s, (c) 4.3 s, (d) 7.2 s, (e) 10 s and, (f) 11.7 s.

We have calculated the prothrombin time and compared the values with those found in past studies [26–29]. Table 1 shows the comparison between the point of care (POC) and lab PT results from the literature [30] and the simulated PT results and different blood volumes (40–100%). The simulated PT and POC PT are similar, and when the volume of the blood is low, both the POC PT and simulated PT are high. Figure 10 shows a graph of the POC PT and simulated PT results for comparison of the difference between the mean POC PT and simulated PT results. When the blood volume is more than 55%, the PT time is less than 16.2 s on average. When the volume of the blood increases the PT time is shorter. When the volume is 100%, the simulated PT time is 12.3 s and the lab POC PT result is 12 s.

Table 1. Comparison between point of care prothrombin time POC PT [30] and simulated PT.

Blood Volume (%)	Mean POC PT (Min, Max) (s)	Mean Lab PT (Min, Max) (s)	Simulated PT (s)
100	12.0 (11.5, 13.0)	11.7 (10.7, 13.4)	12.3
75	14.6 (13.6, 15.9)	13.3 (12.7, 14.6)	14.5
65	16.2 (15.1, 17.4)	14.7 (13.8, 15.4)	15.5
55	20.1 (17.8, 24.3)	16.1 (14.3, 17.3)	21.0
40	41.8 (35.6, 60.6)	21.8 (17.7, 23.4)	21.0

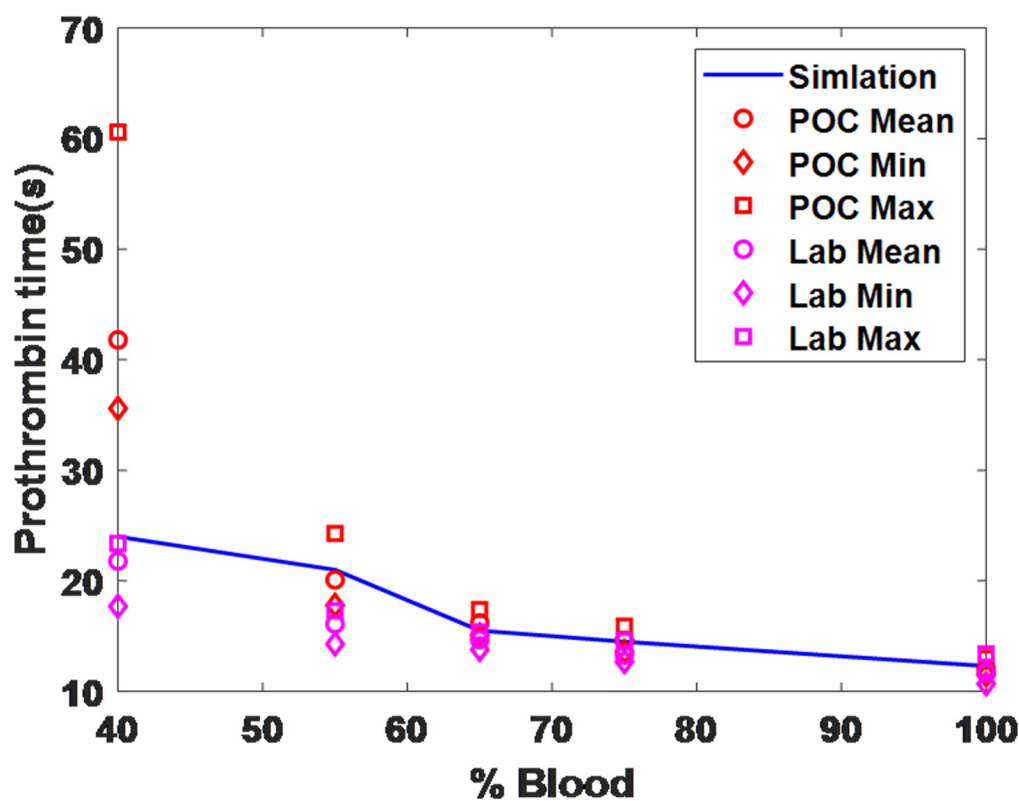


Figure 10. Comparison between mean POC PT, mean Lab POC PT, and simulated PT results.

5. Conclusions

In this study, a genetic algorithm method was used to estimate the various parameters in the chemical reaction to obtain the actual behaviors of blood and anticoagulant in the microchannel. The following conclusions can be drawn:

1. Through simulation, it can be found that the chemical reaction of prothrombin in blood is a factor. When the reaction rate is k_1 , and reaction order n_2, n_3 increase, prothrombin will be quickly depleted, causing the drug to flow to the blood end, but too slow the time of PT is extended. The reaction rate and reaction order can be

obtained more accurately by genetic algorithm. The chemical reaction rate constants indicate that the reaction rate of prothrombin activator is faster than thrombin, fibrin activator is faster than thrombin, and prothrombin activator is faster than fibrin.

2. Predicted by simulation and experimental results, high blood concentration (>65%) is more accurate in predicting PT.
3. In order to observe whether RBCs and WBCs are obstructed in the microchannel, the PT time cannot be accurately and effectively evaluated. Therefore, the dynamic mesh method can clearly determine the time for RBCs and WBCs to pass through the microchannel and can predict the dynamic behavior of blood and coagulants. The white blood cell flow time is 11.7 s and there are no obstructions.

Author Contributions: Methodology, software, formal analysis, investigation, resources, Y.-H.C.; writing—original draft preparation, review and editing, visualization, P.N.I.; supervision, project administration, funding acquisition, S.-J.H. All authors have read and agreed to the published version of the manuscript.

Funding: This research was funded by the Ministry of Science and Technology, MOST: MOST 107-2218-E-011-020.

Institutional Review Board Statement: Not applicable.

Informed Consent Statement: Not applicable.

Data Availability Statement: Data available on request due to restrictions eg privacy or ethical. The data presented in this study are available on request from the corresponding author. The data are not publicly available due to their containing information that could compromise the privacy of research participants.

Conflicts of Interest: The authors declare no conflict of interest.

Nomenclature

Nomenclature

V	velocity
m_{ij}	mass from phase i to phase j
X, Y	mass fraction
M_w	molecular weight
P	static pressure
J	diffusion flux
R	net rate of production by chemical reaction
$D_{j,m}$	diffusion coefficient for species j in the mixture
N	number of chemical species in the system
N_r	number of chemical species in reaction r
$\nu_{j,r}$	stoichiometric coefficient for reactant j in reaction r
$\nu'_{j,r}$	stoichiometric coefficient for product j in reaction r
M_j	symbol denoting species j
$k_{f,r}$	forward rate constant for reaction r
$k_{b,r}$	backward rate constant for reaction r
$C_{k,r}$	molar concentration of each reactant and product species k in reaction r
$\eta_{k,r}$	forward rate exponent for each reactant and product species k in reaction r
$\eta'_{k,r}$	backward rate exponent for each reactant and product species k in reaction r
t	time
g	gravity acceleration
k_1-k_3	chemical reaction rate
n_1-n_5	chemical reaction order
w_1	weighting mass fraction
f_1	objective function coefficient
dA	average mass fraction

Greek letters	
α	volume fraction
β	interphase momentum exchange coefficient
μ	viscosity
τ	stress tensor
ρ	density
Subscripts	
i	phase, species
j, k, l	species
r	reaction

References

- He, S.; Sharpless, N.E. Senescence in health and disease. *Cell* **2017**, *169*, 1000–1011. [[CrossRef](#)] [[PubMed](#)]
- Baumann, K. Cellular senescence: Senescence and reprogramming go hand-in-hand. *Nat. Rev. Mol. Cell. Biol.* **2016**, *18*, 4. [[CrossRef](#)] [[PubMed](#)]
- Anderson, E.L.; Howe, L.D.; Jones, H.E.; Higgins, J.P.; Lawlor, D.A.; Fraser, A. The prevalence of non-alcoholic fatty liver disease in children and adolescents: A systematic review and meta-analysis. *PLoS ONE* **2015**, *10*, e0140908. [[CrossRef](#)] [[PubMed](#)]
- Copplestone, J.A. 11 Bleeding and coagulation disorders in the elderly. *Bailliere's Clin. Haematol.* **1987**, *1*, 559–580. [[CrossRef](#)]
- Saeed, A.; Alsubie, A.; Kumam, P.; Nasir, S.; Gul, T.; Kumam, W. Blood based hybrid nanofluid flow together with electromagnetic field and couple stresses. *Sci. Rep.* **2021**, *11*, 12865. [[CrossRef](#)]
- Saeed, A.; Khan, N.; Gul, T.; Kumam, W.; Alghamdi, W.; Kumam, P. The flow of blood-based hybrid nanofluids with couple stresses by the convergent and divergent channel for the applications of drug delivery. *Molecules* **2021**, *26*, 6330. [[CrossRef](#)]
- Alghamdi, W.; Alsubie, A.; Kumam, P.; Saeed, A.; Gul, T. MHD hybrid nanofluid flow comprising the medication through a blood artery. *Sci. Rep.* **2021**, *11*, 11621. [[CrossRef](#)]
- Korvink, J.; Paul, O. *MEMS: A Practical Guide of Design, Analysis, and Applications*; World Scientific: Singapore, 2010; p. 905.
- Bertsch, A.; Heimgartner, S.; Cousseau, P.; Renaud, R. Static micro-mixers based on large-scale industrial mixer geometry. *Lab. Chip.* **2001**, *1*, 56–60. [[CrossRef](#)]
- Hossian, S.; Ansari, M.A.; Kim, K.Y. Evaluation of the mixing performance of three passive micromixers. *Chem. Eng. J.* **2009**, *150*, 492–501. [[CrossRef](#)]
- Kuo, J.N.; Liao, H.S.; Li, X.M. Design optimization of capillary-driven micromixer with square-wave microchannel for blood plasma mixing. *Microsyst. Technol.* **2007**, *23*, 721–730. [[CrossRef](#)]
- Wong, S.; Ward, M.; Wharton, C. Micro T-mixer as a rapid mixing micromixer. *Sens. Actuators B Chem.* **2004**, *100*, 359–379. [[CrossRef](#)]
- Ahmed, A.M.; Normah, M.G.; Robiah, A. Optimization of an ammonia-cooled rectangular microchannel heat sink using multi-objective non-dominated sorting genetic algorithm (NSGA2). *J. Heat Mass Transf.* **2012**, *48*, 1723–1733. [[CrossRef](#)]
- Palta, S.; Saroa, R.; Palta, A. Overview of the coagulation system. *Indian J. Anaesth.* **2014**, *58*, 515–523. [[CrossRef](#)] [[PubMed](#)]
- MacFarlane, R.G. An enzyme cascade in the blood clotting mechanism, and its function as a biochemical amplifier. *Nature* **1954**, *202*, 498–499. [[CrossRef](#)] [[PubMed](#)]
- Seegers, W.H. Blood clotting mechanisms: Three basic reactions. *Ann. Rev. Physiol.* **1969**, *31*, 269–294. [[CrossRef](#)]
- Madana, V.S.; Basheer, A.A. Computational investigation of flow field, mixing and reaction in a T-shaped microchannel. *Chem. Eng. Commun.* **2021**, *208*, 903–913. [[CrossRef](#)]
- ANSYS. *ANSYS Fluent Theory Guide*; ANSYS Inc.: Canonsburg, PA, USA, 2019.
- Foli, K.; Okabe, T.; Olhofer, M.; Jin, Y.; Sendhoff, B. Optimization of micro heat exchanger: CFD, analytical results and multiobjective evolutionary algorithms. *Int. J. Heat Mass Transf.* **2006**, *49*, 1090–1099. [[CrossRef](#)]
- Amanifard, N.; Narima, N.-Z.; Borji, M.; Khalkhali, A.; Habidoust, A. Modeling and pareto optimization of heat transfer and flow coefficients in microchannel using GMDH types of neural networks and genetic algorithm. *Energy Convers. Manag.* **2008**, *49*, 311–325. [[CrossRef](#)]
- Khan, W.A.; Kadri, M.B.; Ali, Q. Optimization of microchannel heat sinks using genetic algorithm. *Heat Transf. Eng.* **2013**, *34*, 279–287. [[CrossRef](#)]
- Jafari, A.; Mousavi, S.M.; Kolari, P. Numerical investigation of blood flow. Part I: In microvessel bifurcations. *Commun. Nonlinear Sci. Numer. Simul.* **2008**, *13*, 1615–1626. [[CrossRef](#)]
- Jafari, A.; Zamankhan, P.; Mousavi, S.M.; Kolari, P. Numerical investigation of blood flow. Part II: In capillaries. *Commun. Nonlinear Sci. Numer. Simul.* **2009**, *14*, 1396–1402. [[CrossRef](#)]
- Ni, A.; Cheema, T.A.; Park, C.W. Numerical study of RBC motion and deformation through microcapillary in alcohol plasma solution. *Open J. Fluid Dyn.* **2015**, *5*, 26–33. [[CrossRef](#)]
- Houdijk, W.P.M.; van den Besselaar, A.M.H.P. International multicenter international sensitivity index (ISI) calibration of a new human tissue factor thromboplastin reagent derived from cultured human cells. *J. Thromb. Haemost.* **2004**, *2*, 266–270. [[CrossRef](#)]
- Matsuda, T.; Murakami, M. Relationship between fibrinogen and blood viscosity. *Thromb. Res.* **1976**, *8*, 25–33. [[CrossRef](#)]
- Fogel, D. *Evolutionary Computation: Toward a New Philosophy of Machine Intelligence*, 3rd ed.; IEEE Press: Piscataway, NJ, USA, 2006.

28. Yang, C.L.; Huang, S.J.; Chou, C.W.; Chiou, Y.C.; Lin, K.P.; Tsai, M.S.; Young, K.C. Design and evaluation of a portable optical-based biosensor for testing whole blood prothrombin time. *Talanta* **2013**, *116*, 704–711. [[CrossRef](#)]
29. Yang, C.L.; Chiou, Y.C.; Chou, C.W.; Young, K.C.; Huang, S.J.; Liu, C.Y. Point-of-care testing of portable blood coagulation detectors using optical sensors. *J. Med. Biol. Eng.* **2013**, *33*, 319–324. [[CrossRef](#)]
30. Balendran, C.A.; Henderson, N.; Olsson, M.; Lövgren, A.; Hansson, K.M. Preclinical evaluation of point-of-care prothrombin time as a biomarker test to guide prothrombin replacement therapy in coagulopathic bleeding. *Res. Pract. Thromb. Haemost.* **2017**, *1*, 252–258. [[CrossRef](#)]